Supporting Information

Murphy *et al.* 10.1073/pnas.0802743105

SI Methods

Vessel segments per 10× field (Zeiss Axioskop with a ×10 objective; field is ≈1 mm^2) were calculated for three 10-μm sagittal sections per animal, adjacent to the midline of mutant mice and littermate controls in each of three regions [Cerebellum (Lobule VI), neocortex, and brainstem]. Vessel density reflects vessels with either CD31 staining or lectin perfusion. Perfusion density reflects lectin-perfused vessels. Density values for each region were averaged across three sections. For diameter measurements, images were thresholded, and minimal diameter through the centroid was automatically assessed for all objects in the field with ImagePro software. Objects that did not meet a minimal requirement or were clearly nonvascular artifacts were not included. Diameter measurements were also averaged across three sections per region and summed by size into three categories. The ratio of vessels within each size category to the total number of vessels was used to compare vessel sizes in control and mutant brains. The percent change in these ratios in the mutant brain relative to the control brain was determined for each brain region.

A two-tailed Student's *t* test, assuming equal variation, was performed to determine the significance of the decrease in vessel density of mutants relative to controls. A two-tailed Student's *t* test, assuming equal variation, was performed to determine the significance of the decrease in the ratio of small vessels, and the increase in the ratio of medium and large vessels, in the mutant brain. Linear regression was performed using STATA-IC to determine the strength of the correlation between the change in vessel density and the change in the ratio of large vessels (>50 μm), relative to controls, across all regions of the brain.

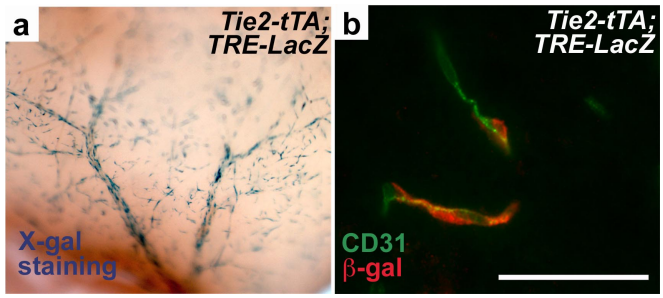

Fig. S1. tTA was active specifically in endothelial cells by reporter assay. A β-gal reporter of tTA activity was detected by whole-mount X-gal staining (*a*) and immunostaining of sections with anti-β-gal (*b*) in a P12 brain. (Scale bar, 50 μm.)

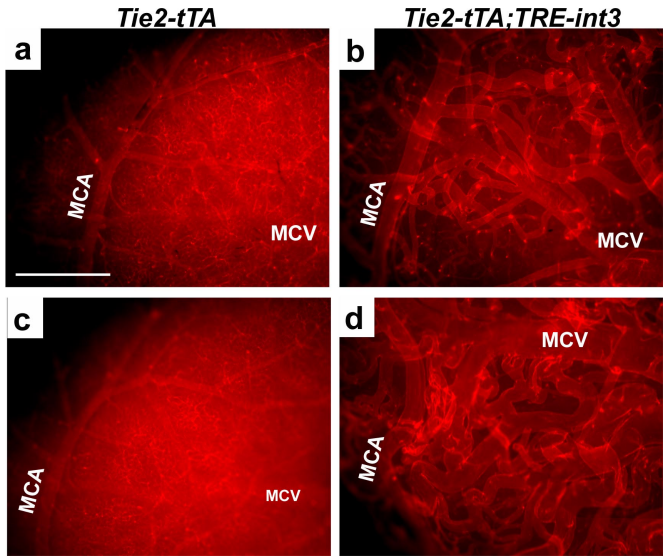

Fig. S2. Endothelial Notch activation induces enlargement of cerebral arteries and veins. Note the enlargement of both the middle cerebral artery (MCA) and the middle cerebral vein (MCV) in lateral images of both severely affected mice (*b* and *d*). These changes were not seen in their littermate controls (*a* and *c*). (Scale bar, 1 mm.)

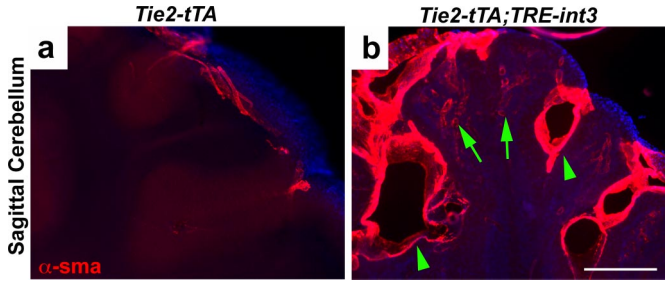

Fig. S3. Smooth muscle coverage of enlarged vessels revealed by anti-smooth muscle α-actin (α-SMA) staining of both large vessels (green arrowheads) and small vessels (green arrows) in a 100-μm thick mutant section (*b*), but not in control section (*a*). (Scale bar, 400 μm.)

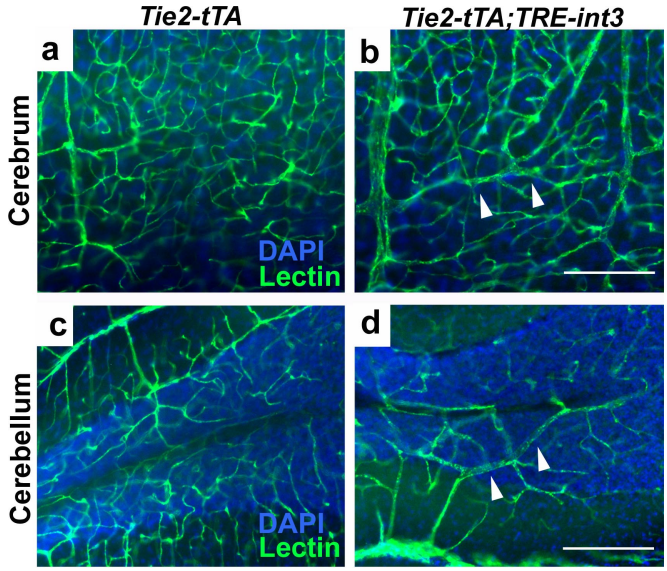

Fig. S4. Vessel enlargement (arrowheads), shown by FITC-labeled lectin perfusion in sagittal section, occurred before signs of abnormalities, including hemorrhage, neuronal cell death, or ataxia in mutants (*b* and *d*) but not in littermate controls (*a* and *c*). (Scale bar, 200 μm.)

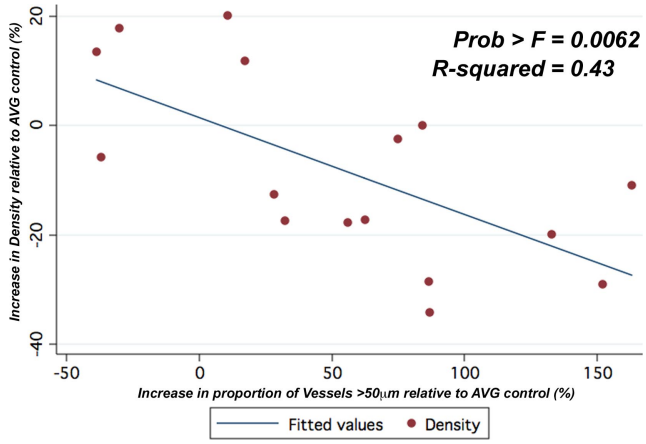

Fig. S5. The increase in the proportion of large vessels in *int3* expressing mutant mice is correlated with a decrease in vessel density. This is shown by a scatter plot and linear regression of the relationship between the percent change in vessel density (relative to average controls in that particular region of the brain) and the percent change in the proportion of vessels >50 μm (relative to average proportion, in control mice, in that particular region of the brain). Each point represents a particular brain region of a mutant mouse, averaged across three sections. Four regions were assessed in three mice, and two regions were assessed in two mice.